Functional Group Analysis of Evaporation and Liquid Combustion of Jet-A and Its Surrogate Fuel Based on Quantitative FT-IR Measurements

Yu Cheng Liu[1] and Brandon Walker[2]
University of Michigan - Flint, Flint, MI, 48502, U.S.A.

This paper reports the evaporation and combustion experiments of small amounts of pool liquid fuel and the preliminary quantification of functional groups including: CH_2, CH_3, t-butyl, iso-propyl and mono-substituted aromatics using light absorbance in the wave number range of 400-4000 cm^{-1}. The goal was to develop a method that formulates evaporation characteristics for a complex real fuel and use the results to establish a surrogate's evaporation rate associated with real fuel's functional group evaporation rates. Jet-A (POSF-4658) was selected as the real fuel target in this study and a simple mixture of n-decane/iso-octane/toluene was selected to be the surrogate. The experiments included boiling and a pool fire test of 10 mL liquid fuel samples in a Petri dish. The fuel sample liquid mass was recorded before and after each experiment and the liquid fuel samples were collected using a needle at the end of each experiment. The attenueated total reflection (ATR) module of a Fourier Transform infrared (FT-IR) spectrometer was used to facilitate a large number of liquid measurements. The correlation between concentration and transmittance of each functional group was provided by simple mixtures with known compositions. Results show that the evaporation characteristics of Jet-A and the surrogate mixture are extremely different in terms of time evolution of functional group concentrations and total time. Therefore it suggests the evaporation feature of the surrogate mixture itself is less useful to modeling the evaporation of Jet-A. Moreover, the analyses show that the functional group evolutions during evaporation and pool fire experiments of Jet-A were very similar suggesting the functional group consumptions from liquid combustion may be represented by evaporation.

Nomenclature

C	=	concentration in the liquid sample
l	=	optical path length for Beer-Lambert Law
I	=	transmittance with samples
I_o	=	transmittance without samples
σ	=	cross section for Beer-Lambert Law

I. Introduction

LIQUID hydrocarbon fuels have been used for aerospace propulsion since the late 1800s and the demand will continue to increase for decades to come[1,2]. A large portion of these fuels are derived from the distillation process of crude oil and other liquid fuels with demonstrated potential are from synthesis of bio-feedstock[3-6]. The composition of these fuels are usually very complex and thus it has been difficult to develop a model that details the behaviors that are critical to its use and further design. A surrogate fuel is a simple mixture designed to emulate

---

[1] Assistant Professor, Department of Computer Science Engineering and Physics, Murchie Science Building 207, 303 E. Kearsley St., Flint, MI 48502, AIAA Member.
[2] Undergraduate Stundent, Department of Computer Science Engineering and Physics, Murchie Science Building 207, 303 E. Kearsley St., Flint, MI 48502.

some behaviors, if not all, of complex fuels so that behavioral prediction of the real complex fuel can be realized through surrogate simulation without having to deal with the much more complex composition of the real fuel.

Some surrogate fuels are proposed to match jet fuel's gas phase combustion[7-11]. The selection of surrogate fuel components and their compositions have been directed to match the carbon numbers and general functional groups[9]. More specific and thorough considerations may include the process of matching the derived cetane number (DCN), hydrogen to carbon ratio (H/C), molecular weight (MW), and threshold sooting index (TSI)[12,13]. A series of surrogates has been developed based on the properties of Jet-A (POSF-4658) and tested in several gas phase combustion utilities (shock tube, counter flow flame, variable pressure flow reactor, and rapid compression machine…etc) to demonstrate the methodology[12,13]. The results from those gas phase combustion experiments show fairly good agreement between Jet-A and the surrogates. More recent advances include the nuclear magnetic resonance (NMR) results[14] that indicate more details of fuel functional groups in the process of formulating surrogate composition.

As the fuel is usually injected in the practical combustion systems as a liquid phase, the local liquid-vapor equilibrium at the liquid surface and the rate of different species being released from the liquid should play a very substantial role in a multi-phase combustion process. Due to the fact that each component in a mixture has its distinct volatility and equilibrium parameter with various other components, developing an evaporation surrogate for a real complex fuel like Jet-A may be as equally challenging as developing a combustion surrogate. A more mature area that is relevant to the problem here is the distillation of real complex fuels[10,15,16]. While the classification and quantification of fuel distillates at different distillation volume fraction provides very valuable information for the evaporation of complex fuels, there has not been a consensus regarding the specific properties for a surrogate to match with the target fuel for evaporation purposes. Moreover, the question that motivated this study was whether the information obtained from distillation can be carried over to the evaporation during liquid combustion. Namely, as the preferential evaporation of fuel components in a mixture is a well-observed phenomenon, the present study attempts to discover the preferential consumption of particular species or functional groups during liquid combustion that may alter the results of preferential evaporation from fuel distillation experiments. Figure 1 illustrates such a consideration.
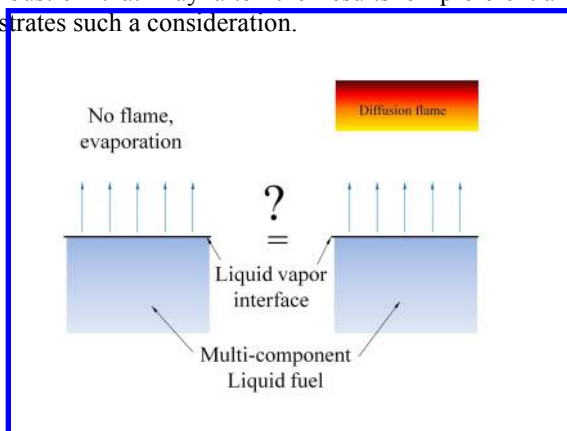

Figure 1. Illustration of pure evaporation or distillation (left) and the fuel vaporization with diffusion flame (right).

Among the considerations of developing a gas phase combustion surrogate, the amount of similar functional groups (or radicals[13]) provided by the prevaporized surrogate is the critical factor in order to mimic the combustion kinetics in gas phase. Similarly, it is important to control the evaporation rate of each surrogate component such that similar amounts of similar functional groups are released into gas phase to creating a similar radical pool in gas phase. The concentration of important functional groups from either liquid or gas samples during evaporation or liquid combustion becomes a piece of necessary information. The quantification of these functional groups may be realized by analyzing infrared spectra of the fuel sample obtained using Fourier-transform infrared (FT-IR) spectroscopy. Note that gas chromategraph with mass spectroscopy (GC-MS) may be able to give very detailed identification for the fuel components, but for surrogate development purposes functional group lumping is more important, which may not require detailed GC-MS information.

FT-IR spectra have been used in several combustion experiments to reveal the concentration of combustion gases like CH_4, C_2H_4, CH_2O, H_2O …etc. at high temperature and pressures[17,18]. Techniques of laser absorption have been used to detect hydrocarbon fuel concentration using the strong absorption of gaeous hydrocarbons at 3.39 μm (~2950 cm^{-1})[19] and more recently it was found possible to detect iso-butene using the absorption of a much longer wavelength 11.3 μm (885 cm^{-1})[20] generated by a wavelength tunable quantum cascade laser. Typical FT-IR measurements provide the light absorbance over a wider range of wavelength (μm) or wave number (cm^{-1}). In particular, the attenuated total reflection (ATR) module of a FT-IR can be used as a very convient platform for room temperature liquid samples as it does not require a large amount of liquid for measurement and is easy to clean and change from sample to sample. Figure 2 shows the FT-IR ATR results for Jet-A (black) and its surrogate (mixture of decane, iso-octane, and toluene) (red). The peak intensities are presented as absorbance with 1.0 being total

absorption and 0.0 as total transmission. As shown in Fig. 2, there are clearly identifiable peaks in the range of 2800-3000 cm^{-1}, 1300-1500 cm^{-1}, and 600-900 cm^{-1} for both Jet-A and the surrogate. The corresponding vibration and stretch mode of these peaks will be discussed in the next section. The spectra show in Fig. 2 provide an opportunity for quantifying various functional groups (each as a lumped group) in a fuel mixture regardless of the variety of combination of those groups. The evolution of these peaks can be used to reveal the preferential evaporation in terms of the amount of functional groups.
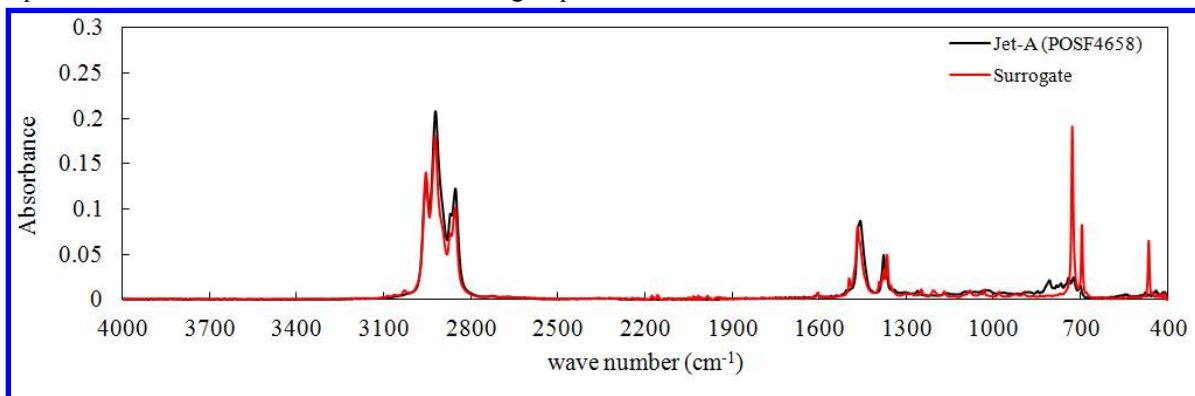

Figure 2. FT-IR ATR spectra of liquid Jet-A (POSF-4658) (black) and its surrogate (n-decane/iso-octane/toluene 0.427/0.33/0.243 mole fraction) (red).

In this study, we report the evaporation of a 10 mL quantity of liquid Jet-A and the surrogate at its boiling condition and the pool fire of the same amount of liquid Jet-A. Noted that the pool fire of the surrogate may not be relevant because the main focus here is to match the experimental results of Jet-A.

II. Experimental Methods

A. Evaporation experiments

Comprating with typical distillation experiments that deal with more than 500 mL of liquid and require a longer experiment time, the evaporation experiments reported here use very small amounts of liquid fuels (10 mL). Sampling from the same batch of liquid during boiling may introduce artifacts to the distillate weight percentage so a set of experiments with different end times was performed and the sample was always collected at the end of each experiment.

The simple procedures were developed as follows: 1) weigh an empty Petri dish; 2) measure 10 mL liquid fuel using a graduate cylinder; 3) pour the fuel into the Petri dish and weigh it; 4) put the dish containing 10 mL liquid fuel onto a hot plate (around 260°C, it took less than 2 seconds for the liquid fuel to reach a boiling state); 5) after a designed time t, terminate the experiment by removing the dish from the hot plate to the precision scale and measure the weight; 6) use a needle to quickly extract the liquid sample (around 2 mL) and seal the needle for later FT-IR analysis. Steps 5) and 6) were performed within 10 seconds to minimize uncertainties due to continuing evaporation of fuel on the scale. Figure 3 (a, b, c, d, e) illustrates the above procedures for evaporation experiments. All the above procedures were realized in a ventilation hood.

For the surrogate fuel (n-decane/iso-octane/toluene with a molar ratio of 0.427/0.33/0.243[12], or a volumetric ratio of 0.51/0.33/0.16[21]) and the Jet-A (POSF-4658) tested in this study, the total evaporation time was less than 3 minutes. Therefore the evaporation time t for separate experiments was designed to be 0s, 20s, 40s, 60s, ...at a 20s increment until the fuel was completely vaporized near 180s. The chemicals for surrogate components were obtained from Sigma-Aldrich with purity higher than 99%. The Jet-A (POSF-4658) was obtained from the Wright Patterson Air Force Base of USA.

Because there exists small differences between the initial fuel mass from run to run, the results will be shown in a base of vaporized mass percentage. The readability of the scale (Sartorius Corporation, SECURA613-1S) was 0.001 g. The weight loss during the 10 second of weighing and sample extraction at the end of experiment was usually less than 0.05 g, which is about 0.6% of a 10 mL (around 8 g) fuel.

B. Combustion Experiments

The combustion experiments reported in this study were simple pool fire experiments that consumed the 10 mL liquid Jet-A fuel in the Petri dish. The experimental procedures were as follows: 1) same as 1) to 3) in evaporation

American Institute of Aeronautics and Astronautics

experiments; 2) preheat the fuel using the hot plate (it took less than 2 seconds to reach a boiling state); 3) place the dish on a room temperature plate and ignite the hot liquid using a propane flame (note that Jet-A liquid is difficult to ignite using a propane flame at room temperature); 4) same as 5) to 6) in evaporation experiments for sample collection. The pool fire flame consumed the liquid fuel (Jet-A) within 3 minutes and the incremental time interval between different runs was 20 seconds. Figure 3 (a, b, f, g, d, e) illustrates the procedures for a pool fire experiment. All the above procedures were completed in a ventilation hood.

In combustion experiments, the flame provided the heat to quickly vaporize the liquid fuel therefore the dish did not need to stay on the hot plate during the combustion process. When the hot fuel was being weighed at the end of experiment, the weight variation within the 10 second window of weighing and sample extraction was similar to the evaporation case since the fuel was also near its boiling point.
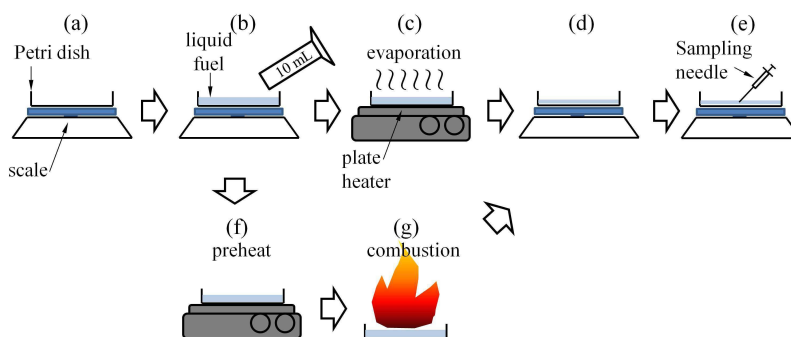

Figure 3. Illustration of the experimental procedures (a) weigh the empty Petri dish, (b) add 10 mL of liquid fuel and weigh it, (c) place the dish on a hot plate for evaporation experiments, (d) weigh the fuel and Petri dish after time t, (e) collect the liquid fuel sample using a needle, (f) preheat the fuel, (g) ignite the preheated fuel for combustion experiments. Steps for an evaporation experiment are a, b, c, d, e, and for an combustion experiment are a, b, f, g, d, e.

C. FT-IR Anlayses

The samples extracted from the evaporation and combustion experiments were tested using the ATR module of a FT-IR spectrometer (Thermo Scientific Nicolet iS50). The ATR measurement does not require salt windows or a cell to perform the analysis and only requires very little amount of liquid sample on the analysis surface. The measurements for liquid samples were performed at room temperature and atmospheric pressure to avoid peak broadening effects[22]. The volume of samples (around 2 mL) collected from the experiment were much more than what is required by an ATR analysis. After the background peaks were collected, a few droplets were placed on the ATR window surface. The scanning range was from 400 cm^{-1} to 4000 cm^{-1} with a reolustion of 0.4 cm^{-1}. All the absorbance spectra shown in this study are the averaged data from 5 individual scans of the same sample.

The raw data from FT-IR is the absorbance in a function of wave number (cm^{-1}). Table 1 lists the wave numbers of prominent peaks that are relevant to the functional groups of interests in this study.

Table 1. A list of absorbance wave numbers (cm^{-1}) and their corresponding light absorption modes (ν: stretch vibration, δ: bending vibration, subscript s: symmetrical, as: asymmetrical.)[23]

Light absorption mode	Wave number (cm^{-1})
ν_{as} CH_3 (two C-H extending, one contracting)	~2954
ν_{as} CH_2	~2921
ν_s CH_3 (all three C-H extending and contracting in phase)	~2870
ν_s CH_2	~2853
δ_s CH_2	~1465
δ C-H for t-butyl group	~1393
δ C-H for iso-propyl group	~1365
Aromatic C-H out of plane bending	600-900

American Institute of Aeronautics and Astronautics

In order to convert the absorbance to an absolute concentration, FT-IR measurements were also performed for a various combination of surrogate components, i.e. decane (D), iso-octane (S), and toluene (T), D1S1, D1S2, D2S1, S1T1, S1T2, S2T1, D1T1, D1T2, D2T1, D1S1T1 (the numbers stand for volumetric ratios) and the three component surrogate mixture described in evpoartion experiment. Based on the Beer-Lambert Law of light absorption:

$$I/I_o = \exp(-\sigma \times l \times C) \tag{1}$$

According to Eq. (1), ln(I) should be proportional to concentration C. The absolute concentration of each functional group is the product of component concentration (mole/mL) and the number of functional groups listed in Table 2. Figure 4 shows the graph of ln(I) vs. functional group concentration C. Most data collected formed clear straight lines except for the more scattered data from CH_3, 2954 cm^{-1} and CH_3, 2872 cm^{-1}. This is speculated to be the probability of various stretching motions (cf. Table 1) that may slightly vary with the adjacent molecular structure. One other possibility is that the absolute peak intensity may be a result of a sum of neighbor overlapping peaks, especially for the region of 2800-3000 cm^{-1}.

Table 2. A list of absorbance wave numbers (cm^{-1}) and their corresponding light absorption modes.

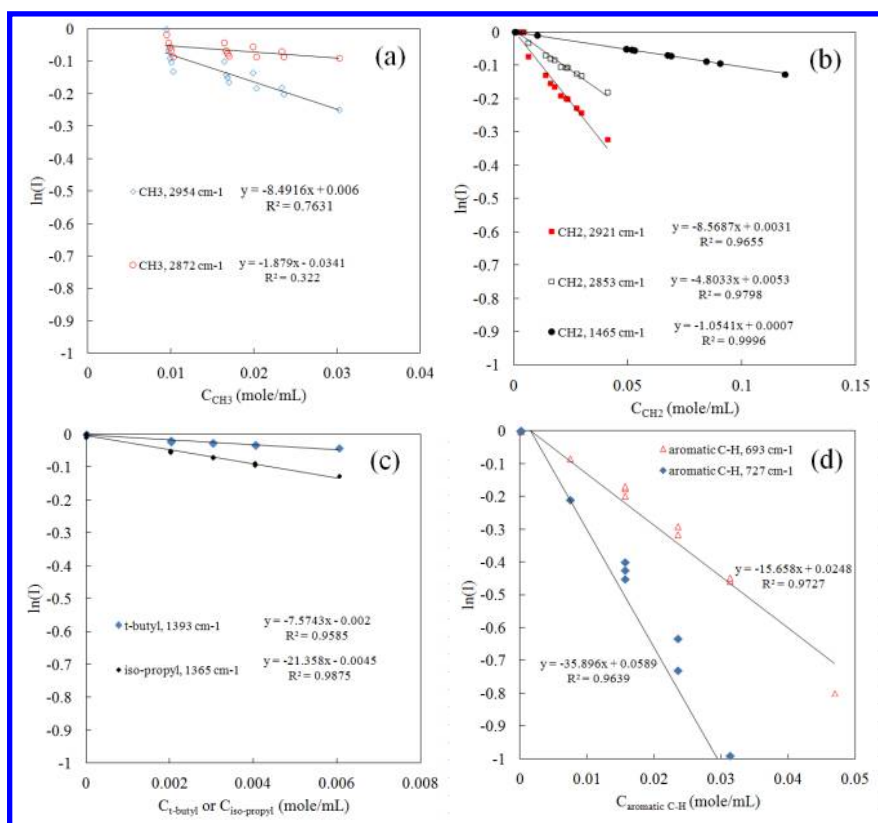|	CH$_2$	CH$_3$	t-butyl C	iso-propyl C	Aromatic CH
Decane	8	2	0	0	0
Iso-octane	1	5	1	1	0
Toluene	0	1	0	0	5

Figure 4. ln(I) vs. functional group concentration (a) CH$_3$ at 2954 and 2872 cm^{-1}, (b) CH$_2$ at 2921, 2853, and 1465 cm^{-1}, (c) t-butyl at 1393 cm^{-1} and iso-propyl at 1365 cm^{-1}, (d) aromatic C-H at 727 and 693 cm^{-1}. The absorbance data come from various volumetric combination of n-decane, iso-octane, and toluene.
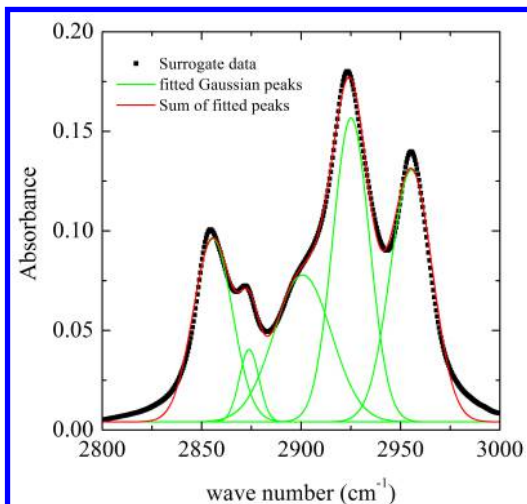
Figure 5. FT-IR ATR spectra of the surrogate mixture (black data) in the range of 2800-3000 cm^{-1} and the Gaussian peak fittings (green curves) and the sum of fitted peaks (red curves).

Figure 5 shows five Gaussian peaks fitted to the spectra of the surrogate mixture in the range of 2800-3000 cm^{-1} using the multi-peak fittings tool of Origin Pro 8. The graph suggests that the observed peak intensity (black data) near 2853 cm^{-1} is very close to the local fitted green curve. This means directly using the FT-IR data without fittings would give nice correlations since the peak at this location is more isolated and not affected by other peaks. On the contrary, the fitted peak around 2872 cm^{-1} is almost one half of the observed intensity. As a result, the observed intensity at near 2872 cm^{-1} may have contribution from the broadening of neighbor peaks leading to a set of more scattering data (with a very low R^2 value, 0.322). The calibration for CH_3 concentration would have to come from the data from 2954 cm^{-1}. Among all CH_2 data (Fig. 5b), the one from 1465 cm^{-1} provides the best R^2 value and the 1465 cm^{-1} is also more isolated than the ones near 2900 cm^{-1}. Therefore the calibration for CH_2 in the later discussion is provided by the linear fit of 1465 cm^{-1} in Fig. 4b. Note that the correlations of t-butyl and iso-propyl (Fig. 4c)
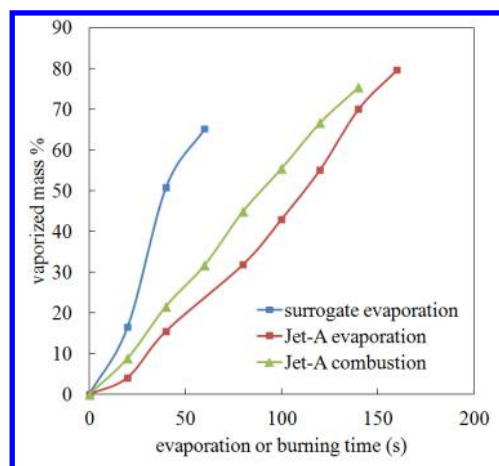
come exclusively from the concentration of iso-octane. Inclusion of other chemicals may be considered for the calibration purposes in the future. The correlations provided in Fig. 4 should be able to handle a mixture of n-decane, iso-octane, and toluene. However, in the hope of covering most functional groups identified from the Jet-A spectrum using surrogate fuel components, there are still some aromatic functional groups that can not be solely covered by toluene. For instance, aromatics with various benzene substitutions cause the inconsistency found in Fig. 2 in the range of 600-900 cm^{-1}. This issue will be briefly discussed in the next section.

III. Results and Discussions

The evaporation experiments were carried out for both Jet-A and the 3 component surrogate (cf. Fig. 2). Figure 6 shows the time evolution of vaporized mass percentage for the evaporation of Jet-A and its surrogate, as well as Jet-A combustion. The results suggest that the evaporation rate of surrogate was much faster than that of Jet-A. The combustion of Jet-A consumes the fuel at a very similar rate compared to evaporation.

Figure 7 shows the absorbance peaks from evaporation experiments of the surrogate with selected time at the three wave number ranges of interests: (a) 2800-3000 cm^{-1}, (b) 1300-1550 cm^{-1}, (c) 600-800 cm^{-1}. As evaporation time increases, there are significant and consistent increases in the peak intensities of 2853 cm^{-1} and 2921 cm^{-1} (both representing CH_2). A slight decrease of CH_3 concentration can be found at 2954 cm^{-1}. The peak at 1365 cm^{-1} (iso-propyl group) (Fig. 7b) decreases with time. This trend exclusively indicates that the amount of iso-octane in the liquid mixture decreases during evaporation. The weakening peak at 693 cm^{-1} in Fig. 7c suggests the toluene concentration decreases over time. It may not be necessary to discuss all the peaks that exhibit changes in Fig. 7 because only one peak is needed for a particular functional group to convert peak intensities to concentration.

Figure 6. Time evolution of vaporized mass percentage for evaporation of Jet-A and its surrogate and the combustion of Jet-A.
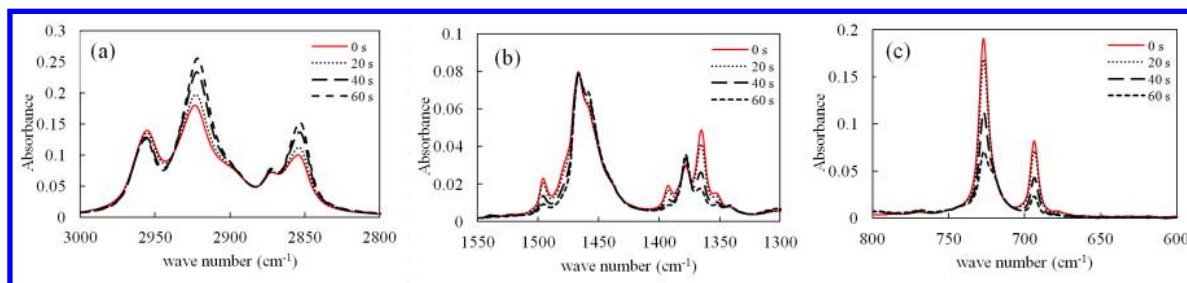
Figure 7. Evolution of absorbance peaks from the evaporation experiments of the surrogate fuel: (a) 2800-3000 cm^{-1}, (b) 1300-1550 cm^{-1}, (c) 600-800 cm^{-1}.

Figure 8 shows the results from evaporation experiments of Jet-A in a similar fashion as in Fig. 7. It is quite obvious that peak intensities in Fig. 8 stay relatively constant compared to the surrogate fuel peaks shown in Fig. 7. As there are only three components in the surrogate mixture, the evaporation is only governed by the phase equilibtrium between n-decane, iso-octane, and toluene. As n-deacne is elected to be the least volatile component in the surrogate, the evaporation is strongly in favor of iso-octane and toluene turning into significant decrease in peak intensities of iso-propyl (1365 cm^{-1}) and aromatic C-H (693 cm^{-1}) shown in Figs. 7b and 7c. The evaporation time of the surrogate was around 60s where on the contrary, Jet-A consists of chemical compounds with a boarder range of carbon numbers and therefore volatility.
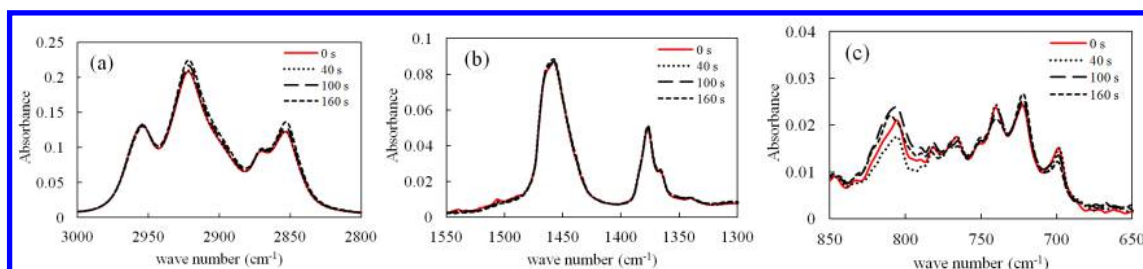

Figure 8. Evolution of absorbance peaks from the evaporation experiments of Jet-A (POSF-4658): (a) 2800-3000 cm^{-1}, (b) 1300-1550 cm^{-1}, (c) 600-800 cm^{-1}.

Figure 9 shows the evolution of absorbance peaks from Jet-A combustion experiments. Interestingly, the functional groups consumption shown in the range of 1300-3000 cm^{-1} by combustion (Fig. 9a and 9b) tends to be very similar to the consumption by evaporation (Fig. 9a and 9b). The differences found for aromatics groups (Fig. 8c and 9c) are in the scale of 0.01 of absorbance, which is still very small.
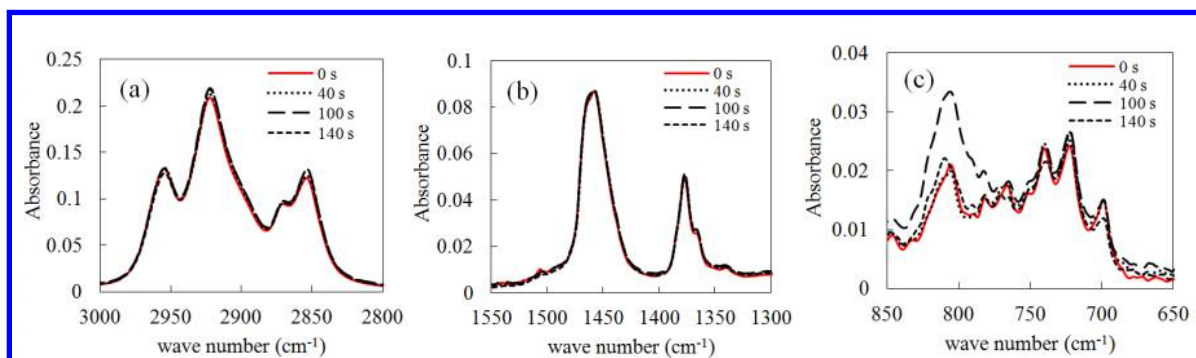

Figure 9. Evolution of absorbance peaks from the combustion experiments of Jet-A (POSF-4658): (a) 2800-3000 cm^{-1}, (b) 1300-1550 cm^{-1}, (c) 600-800 cm^{-1}.

Figure 10 shows the evolution of functional group concentrations using the absorbance in Figs. 7 to 9 and the correlation developed between peak instensity and concentration (Fig. 4). It is evident that the evpoartion characteristics of the surrogate are very different from that of Jet-A. This would suggest that if we must use this suite of surrogate to match the gas phase combustion, the functional group evaporation rate must be fine tuned to match
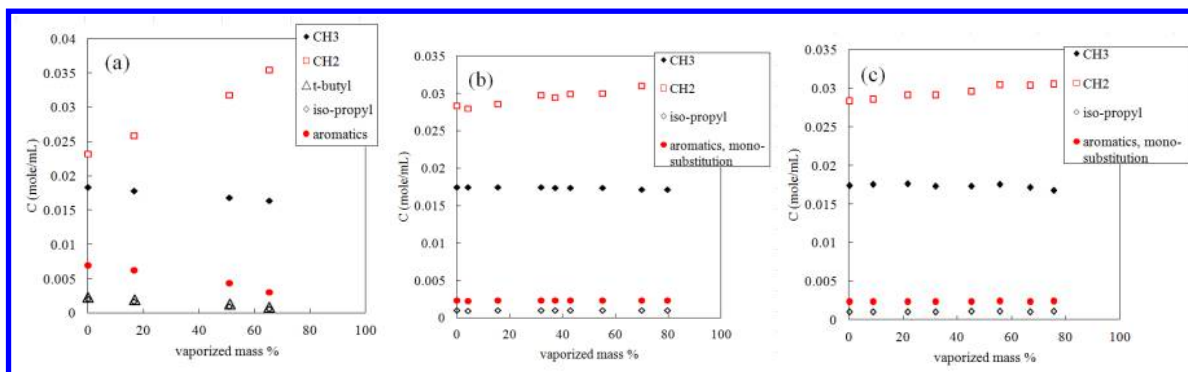
7

American Institute of Aeronautics and Astronautics

Figure 10. Evolution of functional group concentration in the liquid phase (a) surrogate evaporation; (b) Jet-A evaporation; (c) Jet-A burning.

that of Jet-A. In Fig. 10a, the clear increase of CH_2 and decrease of CH_3 indicate that the n-decane concentration is increasing with time. The concentration of t-butyl and iso-propyl are identical because iso-octane is the only compound in the surrogate mixture that provides these functional groups. In other words, these functional group concentrations can be used to represent the concentration of iso-octane in the liquid phase. Similarly, the aromatic concentration must equal to toluene concentration in the surrogate mixture. Figures 10b (Jet-A evaporation) and 10c (Jet-A burning) are almost identical. The functional group concentrations of Jet-A almost remain constant except for slight increase of CH_2. The increase of CH_2 may suggest the hydrocarbons with longer chains possessing higher volatilities tend to remain in the liquid fuel during evaporation or combustion processes.

Note that in both Figs. 10b and 10c the legend of aromatics is followed by "mono-substitution." The reason being that a calibration curve of 727 cm^{-1} (Fig. 4d) was merely derived from toluene concentrations. Toluene has a mono-substituted methyl group on its benzene ring and the absorbance near 727 cm^{-1} as a result of the C-H out-of-plane bending in this molecular configuration. In fact, Jet-A has a much more complex pool of aromatic functional groups so the concentration of which must be obtained by benchmarking different aromatics. Regardless of the functional groups being attached on a benzene ring, different number of substitutions give very distinct peaks.

Figure 11 shows the comparison of FT-IR peaks of the various aromatics tested. It is evident that the Jet-A's aromatic peaks match the peaks from toluene, o-xylene, m-xylene, i.e. mono-, ortho-, and meta- substitutions, respectively. In the future, we attempt to complete the aromatic quantification by comparing the peaks with aromatics with two and three functional group substitution on a benzene ring. Also, attempts will be made to derive the evaporation parameters (e.g., activity coefficients) for surrogate components to match Jet-A's evaporation.
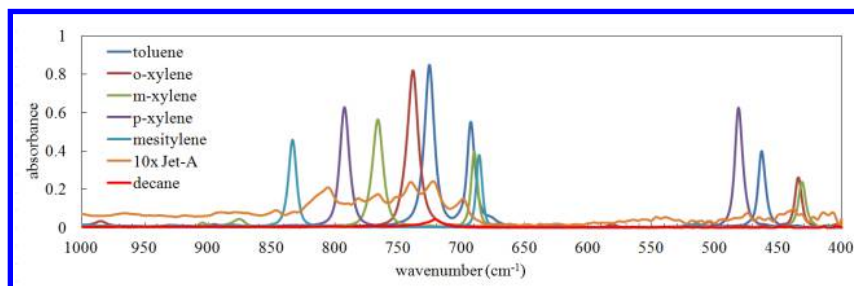

Figure 11. FT-IR ATR absorbance of various aromatics, decane, and Jet-A in 400-1000 cm^{-1} (the aromatic region).

IV. Conclusion

Hot plate evaporation experiments of small liquid amounts (10 mL) of Jet-A and its surrogate were carried out. The total evaporation time of the surrogate was much shorter than that of Jet-A because Jet-A consists of much heavier hydrocarbons that are less volatile. Correlations of FT-IR ATR absorbance and the corresponding concentration have been developed for CH_2 (2853 cm^{-1}), CH_3 (2954 cm^{-1}), t-butyl (1393 cm^{-1}), iso-propyl (1365 cm^{-1}), and mono-substituted aromatics (693 and 727 cm^{-1}) using mixtures of n-decane, iso-octane, and toluene. These correlations are used to reveal the functional group concentrations in liquid from both evaporation and pool fire experiments. The evaporation functional group evolution of the surrogate was very different than that of Jet-A while the results from Jet-A evaporation seem almost identical as from Jet-A burning. Results show that CH_2 concetration

8

American Institute of Aeronautics and Astronautics

increases with time for evaporation of surrogate meaning n-decane is the less volatile component in the surrogate. CH_2 concentration was also found to slightly increase for both Jet-A evaporation and burning. More work needs to be done to match various substitution modes on a benzene ring in order to better represent Jet-A's aromatics.

Acknowledgments

References

[1]Transforming combustion research through cyberinfrastructure. Committee on Building Cyberinfrastructure for Combustion Research, National Research Council, The National Academies Press, ISBN-13: 978-0-309-16387-3, April, 2011. <http://www.nap.edu/catalog.php?record_id=13049>.

[2]Edwards, T.F. "Liquid fuels and propellants for aerospace propulsion: 1903–2003," *AIAA J Propul Power* Vol. 19, No. 6, 1986, pp. 1089–1107.

[3]Rahmes, T.F., Kinder, J.D., Henry, T.M., Crenfeldt, G., LeDuc, G.F., Zombanakis, G.P., Abe, Y., Lambert, D.M., Lewis, C., Juenger, J.A., Andac, M.G., Reilly, K.R., Holmgren, J.R., McCall, M.J., Bozzano, A.G., "Sustainable Bio-Derived Synthetic Paraffinic Kerosene (Bio-SPK) Jet Fuel Flights and Engine Tests Program Results," 9th AIAA Aviation Technology, Integration, and Operations Conference (ATIO) Sep. 21-23, 2009, South California, AIAA 2009-7002.

[4]Blakey, S., Rye, L., Wilson, C.W., "Aviation gas turbine alternative fuels: A review," *Proc. Combust. Inst.* Vol. 33, 2011, pp.2863-2855.

[5]Liu, Y.C., Savas, A.J., Avedisian, C.T., "The spherically symmetric droplet burning characteristics of Jet-A and biofuels derived from camelina and tallow," *Fuel* Vol. 108, 2013, pp. 824-832.

[6]Viljoen, C.L., Van Zyl, V.L., Van Tender, E.H., "Synthetic aviation fuel," *US Patent*, 2013, US 8597493 B2.

[7]Humer, S., Seiser, R., Seshadri, K., "Experimental investigation of combustion of jet fuels and surrogates in nonpremixed flows," *J. Propul. Power* Vol. 27, No. 4, 2011, pp. 847-855.

[8]Holley, A.T., Dong, Y., Andac, M.G., Egolfopoulos, F.N., Edwards, T., "Ignition and extinction of non-premixed flames of single-component liquid hydrocarbons, jet fuels, and their surrogates," *Proc. Combust. Inst.* Vol. 31, 2007, pp. 1205-1213.

[9]Colket, M., Edwards, T., Williams, S., Cernansky, N.P., Miller, D.L., Egolfopoulos, F., Lindstedt, P., Seshadri, K., Dryer, F.L., Law, C.K., Friend, D., Lenhert, D.B., Pitsch, H., Sarofim, A., Smooke, M., Tsang, W., "Development of an experimental database and kinetics models for surrogate jet fuels," 45th AIAA Aerospace Sciences Meeting and Exhibit, Reno, NV, Jan. 8-11, AIAA 2007-0770.

[10]Bruno, T.J., Huber, M.L., "Evaluation of the physicochemical authenticity of aviation kerosene surrogate mixtures. Part 2: analysis and prediction of thermophysical properties," *Energy Fuels* Vol. 24, 2010, pp. 4277-4284.

[11]Jahangirian, S., McEnally, C.S., Gomez, A., "Experimental study of ethylene counterflow diffusion flames perturbed by trace amounts of jet fuel and jet fuel surrogates under incipiently sooting conditions," *Combust. Flame* Vol. 156, 2009, pp. 1799-1809.

[12]Dooley, S., Won, S.H., Chaos, M., Heyne, J., Ju, Y., Dryer, F.L., Kumar, K., Sung, C.-J., Wang, H., Oehlschlaeger, M.A., Santoro, R.J., Litzinger, T.A., "A jet fuel surrogate formulated by real fuel properties," *Combust. Flame* Vol. 157, 2010, pp. 2333-2339.

[13]Dooley, S., Won, S.H., Chaos, M., Heyne, J., Farouk, T.I., Ju, Y., Dryer, F.L., Kumar, K., Hui, X., Sung, C.-J., Wang, H., Oehlschlaeger, M.A., Iyer, V., Iyer, S., Litzinger, T.A., Santoro, R.J., Malewicji, T., Brezinsky, K., "The experimental evaluation of a methodology for surrogate fuel formulation to emulate gas phase combustion kinetic phenomena," *Combust. Flame* Vol. 159, 2012, pp. 1444-1466.

[14]Dussan, K., Dooley, S., Dryer, F.L., Won, S.H., "A nuclear magnetic resonance oriented combustion property regression," 9th U.S. National Combustion Meeting, May 17-20, 2015, Cincinnati, Ohio, paper # 3C06.

[15] Burger, J.L., Bruno, T.J., "Applicatoin of the adcanced distillation curve method to the variability of jet fuels," *Energy Fuels* Vol. 26, 2012, 3661-3671.

[16]Smith, B.L., Bruno, T.J., "Improvements in the measurement of distillation curves. 4. Application to the aviation turbine fuel Jet-A," *Ind. Eng. Chem. Res.*, Vol. 46, 2007, pp. 310-320.

[17]Kock, E.-M, Kogler, M., Pramsoler, R., Klotzer, B., Penner, S., "A high-temperature, ambient-pressure ultra-dry operand reactor cell for Fourier-transform infrared spectroscopy," *Rev. Sci. Instrum.*, Vol. 85, 2014, pp. 084102.

[18]Li, J., Kazakov, A., Dryer, F.L., "Ethanol pyrolysis experiments in a variable pressure flow reactor," *Int. J. Chem. Kinetics* Vol. 33, 2011, pp. 859-867.

[19]Klingbeil, A.E., Jefferies, J.B., Hanson, R.K., " Temperature- and pressure-dependent absorption cross sections of gaseous hydrocarbons at 3.39 µm," *Meas. Sci. Technol.* Vol. 17, 2006, pp. 1950-1957.

[20]Spearrin, R.M., Li, S., Davidson, D.F., Jeffries, J.B., Hanson, R.K., "Higher-temperature iso-butene absorption diagnostic for shock tube kinetics using a pulsed quantum cascade laser near 11.3 μm," *Proc. Combust. Inst.* Vol. 35, 2015, pp. 3645-3651.

[21]Liu, Y.C., Savas, A.J., Avedisian, C.T., "Spherically symmetric droplet combustion of three and four component miscible mixtures as surrogates for Jet-A," *Proc. Combust. Inst.* Vol. 34, 2013, pp. 1569-1576.

[22]Klingbeil, A.E., Jeffries, J.B., Hanson, R.K., "Temperature-dependent mid-IR absorption spectra of gaseous hydrocarbons," *J. Quantitative Spectroscopy & Radiative Transfer* Vol. 107, 2007, pp. 407-420.

[23]Silverstein, R.M., Webster, F.X., Kiemle, D.J., Spectrometric Identification of Organic Compounds, 7th edition, John Wiley & Sons, Inc., 2005, Chap 2.

This article has been cited by:

1. Ke-Feng Song, Guang-Fu Ji, Kotni Meena Kumari, Dong-Qing Wei. 2018. Blending effect between n-decane and toluene in oxidation: a ReaxFF study. *Molecular Simulation* **44**:1, 21-33. [Crossref]